Available online at www.sciencedirect.com

ScienceDirect

Journal of Solid State Chemistry 181 (2008) 276–281

JOURNAL OF SOLID STATE CHEMISTRY

www.elsevier.com/locate/jssc

On the correct spin lattice for the spin-gapped magnetic solid $NH_4CuPO_4 \cdot H_2O$

Hyun-Joo Koo[a,*], Myung-Hwan Whangbo[b]

[a] *Department of Chemistry and Research Institute of Basic Science, Kyung Hee University, Seoul 130-701, Republic of Korea*
[b] *Department of Chemistry, North Carolina State University, Raleigh, NC 27695-8204, USA*

Received 1 August 2007; received in revised form 16 November 2007; accepted 27 November 2007
Available online 5 December 2007

Abstract

$NH_4CuPO_4 \cdot H_2O$ is a spin-gapped compound that has been described in terms of an isolated antiferromagnetic spin dimer model. To explore the origin of this spin gap, we examined the spin exchange interactions of $NH_4CuPO_4 \cdot H_2O$ by performing qualitative spin dimer analysis based on extended Hückel tight binding calculations and also by carrying out quantitative mapping analysis based on first principles density functional theory electronic band structure calculations. Our study indicates that, to a first approximation, the magnetic properties of $NH_4CuPO_4 \cdot H_2O$ should be described by an antiferromagnetic and ferromagnetic alternating chain.

Keywords: Spin dimer analysis; Electronic band structure calculations; Spin exchange interactions; $NH_4CuPO_4 \cdot H_2O$

1. Introduction

The crystal structure and magnetic properties of a layered phosphate $NH_4CuPO_4 \cdot H_2O$ was reported about a decade ago [1]. The magnetic susceptibility of this compound exhibits a spin gap with a pronounced maximum around ~7 K and a very sharp decrease below ~7 K [1]. The observed magnetic susceptibility is well reproduced by an isolated antiferromagnetic (AFM) dimer model with $J/k_B = -4.8\,\mathrm{K}$, $g = 2.16$ and the Curie–Weiss temperature $\theta = -2.7\,\mathrm{K}$ [1], and the structural dimers $(CuO_5)_2$ of $NH_4CuPO_4 \cdot H_2O$ were thought to be the spin dimers [1]. In general, an extended magnetic solid described by an isolated AMF dimer model is often well described by an alternating AFM chain model [2–5]. In such cases, elaborate studies are necessary to know which model is correct. In a magnetic oxide of Cu^{2+} ions, spin exchange interactions between adjacent Cu^{2+} ions may take place through Cu–O–Cu superexchange (SE) paths or Cu–O…O–Cu spuer-superexchange (SSE) paths [6,7]. Goodenough rules [8] enable one to estimate relative strengths of SE interactions. However, SSE interactions can be much stronger than SE interactions [6,7]. The strongly interacting spin exchange paths of a magnetic oxide with Cu^{2+} ions can be quite different from its Cu^{2+} ion arrangement because their magnetic orbitals are anisotropic in shape [6,7]. To properly describe the magnetic properties of a magnetic oxide, it is necessary to examine both SE and SSE interactions on the basis of proper electronic structure considerations [6,7,9,10]. In the present work we explore the origin of the spin gapped behavior of $NH_4CuPO_4 \cdot H_2O$ by performing spin dimer analysis based on extended Hückel tight binding (EHTB) calculations [6,7] and also by carrying out mapping analysis based on first principles density functional theory (DFT) electronic band structure calculations [6,9,10].

2. Spin exchange paths

The building blocks of this compound are CuO_5 square pyramids and PO_4 tetrahedra [1]. Each Cu^{2+} ion is coordinated to four PO_4 tetrahedra and one H_2O to form a distorted CuO_5 square pyramid, and such CuO_5 square pyramids share edges to form $(CuO_5)_2$ dimers. In each layer of $NH_4CuPO_4 \cdot H_2O$, $(CuO_5)_2$ dimers are crosslinked by PO_4 tetrahedra through corner-sharing, and such layers

---

*Corresponding author. Fax: +82 2 966 3701.
E-mail address: hjkoo@khu.ac.kr (H.-J. Koo).

0022-4596/$ - see front matter © 2007 Elsevier Inc. All rights reserved.
doi:10.1016/j.jssc.2007.11.033

are separated by NH_4^+ cations. The arrangement of $(CuO_5)_2$ dimers in a layer of $NH_4CuPO_4 \cdot H_2O$ is schematically shown in Fig. 1. There are four spin exchange paths J_1-J_4 to consider between adjacent spin sites. The spin dimers associated with these spin exchange interactions are depicted in Fig. 2. The J_1 is an SE interaction, while J_2–J_4 are SSE interactions. The geometrical parameters associated with these spin exchange paths are summarized in Table 1.

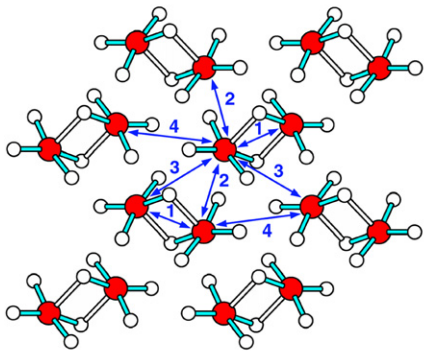

Fig. 1. Schematic representation of a layer of $(CuO_5)_2$ dimers in $NH_4CuPO_4 \cdot H_2O$ and the four spin exchange paths. The numbers 1–4 represent the SE path J_1 and SSE paths J_2, J_3, J_4, respectively. The red and white circles represent Cu and O, respectively. The cyan cylinders of each distorted CuO_5 square pyramid represent four short Cu–O bonds.

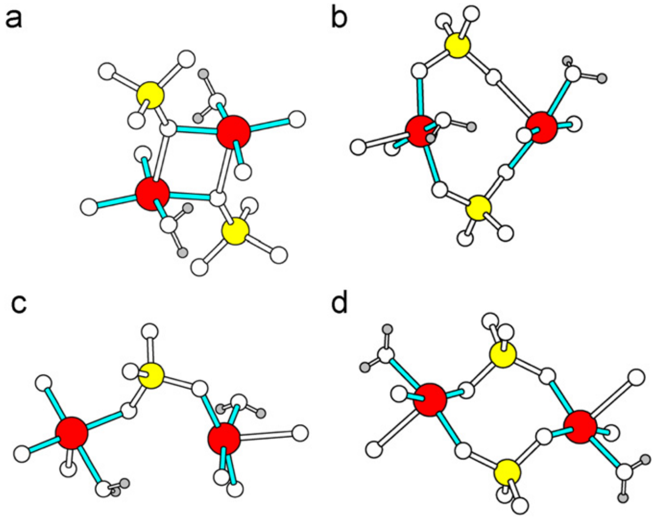

Fig. 2. Spin dimers associated with the spin exchange paths J_1–J_4. The yellow and small gray circles represent the P and H atoms, respectively.

Table 1
Geometrical parameters associated with the SE and SSE paths in $NH_4CuPO_4 \cdot H_2O$[a]

Path	Cu…Cu	Cu–O	∠Cu–O–Cu
(a) SE			
J_1	3.097	1.947, 2.365	91.3

Path	Cu…Cu	Cu–O	O…O	∠Cu–O…O
(b) SSE				
J_2	3.798	1.956, 1.947	2.536	114.6, 88.2
		2.365, 1.918	2.500	121.2, 87.1
J_3	4.706	1.947, 1.918	2.500	141.5, 87.1
J_4	4.775	1.918, 1.956	2.515	135.8, 107.4
		1.956, 1.918	2.515	107.4, 135.8

[a] The bond distances are unit of Å, and the bond angles are unit of degrees.

3. Qualitative spin dimer analysis

In general, a spin exchange parameter J is written as $J = J_F + J_{AF}$ [11], and the ferromagnetic term J_F (>0) is a small positive number so that the spin exchange becomes ferromagnetic (i.e., $J>0$) only when the AFM term J_{AF} (<0) is negligibly small in magnitude. Thus, AFM spin exchange interactions (i.e., $J<0$) can be discussed by focusing on the AFM terms J_{AF} [6,7,11]. In spin dimer analysis based on EHTB calculations, the strength of a spin exchange interaction between two spin sites is estimated by considering only the AFM contribution J_{AF} to the spin exchange [6]:

$$J_{AF} \approx -\frac{(\Delta e)^2}{U_{eff}}, \tag{1}$$

where the (Δe) term refers to the energy split that results when the magnetic orbitals associated with the two spin sites of a given spin dimer interact, and U_{eff} is the effective on-site repulsion that is essentially a constant for a given compound. The magnetic orbital of the distorted CuO_4 square planar unit found in $NH_4CuPO_4 \cdot H_2O$ is presented in Fig. 3, in which the Cu $3d_{x^2-y^2}$ orbital is combined out-of-phase with the $2p$ orbital of each surrounding O ligand. In the present work, the $(\Delta e)^2$ values for various spin dimers are evaluated by performing EHTB calculations [12]. For a variety of magnetic solids of transition metal ions, it has been found that their magnetic properties are well described by the $(\Delta e)^2$ values obtained from EHTB calculations, when both the d orbitals of the transition

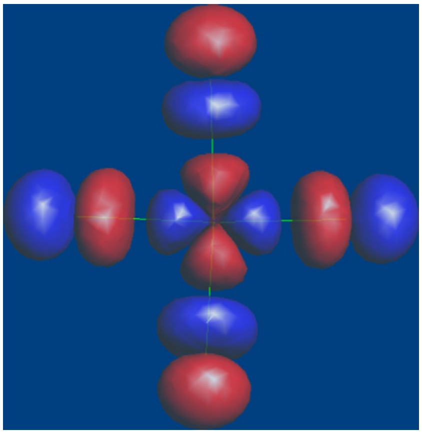

Fig. 3. Magnetic orbital of each distorted CuO_4 square planar unit in $NH_4CuPO_4 \cdot H_2O$.

metal ions and the *s*/*p* orbitals of its surrounding ligands are represented by double-zeta Slater-type orbitals (DZ-STO) [13]. The atomic parameters used in our calculations are summarized in Table 2. The radial part of a DZ-STO is expressed as r^{n-1} $[c_1 \exp(-\zeta_1 r) + c_2 \exp(-\zeta_2 r)]$, where n is the principal quantum number, and the exponents ζ_1 and ζ_2 describe contracted and diffuse STOs, respectively (i.e., $\zeta_1 > \zeta_2$). The diffuse STO provides an orbital tail that enhances overlap between O atoms in the O…O contacts of the Cu–O…O–Cu SSE paths. The $(\Delta e)^2$ values are affected most sensitively by the exponent ζ_2 of the diffuse O 2*p* orbital. The ζ_2 values taken from the results of electronic structure calculations for neutral atoms [13] may not be diffuse enough to describe O^{2-} ions. To make the O 2*p* orbital more diffuse, the ζ_2 value should be reduced. To assess how the diffuseness of the O 2*p* orbital affects the relative strengths of the SSE interactions, we replace ζ_2 with $(1-x)\,\zeta_2$ and calculate the $(\Delta e)^2$ values for three values of x, i.e., 0.00, 0.05 and 0.10.

To examine the effect of the PO_4 bridging units on spin exchange interactions, we calculated the $(\Delta e)^2$ values with and without the PO_4 units in the spin dimers (Fig. 2). The $(\Delta e)^2$ values calculated without the PO_4 units are summarized in Table 3a, and those with the PO_4 units in Table 3b. In the calculations without the PO_4 units, the SSE interaction J_4 dominates hence leading to isolated spin dimers (Fig. 4), and this finding does not depend on the value of x. However, a quite different picture emerges from the calculations with the PO_4 units. When $x = 0.00$, the SSE interaction J_3 dominates leading to uniform chains along the *b*-direction (Fig. 4a). This result is inconsistent with the spin gapped behavior of $NH_4CuPO_4 \cdot H_2O$, because a uniform Heisenberg AFM chain does not have a spin gap [11b]. As the O 2*p* orbital becomes more diffuse, the strength of the SE interaction J_1 increases eventually becoming stronger than the SSE interaction J_3. The resulting spin lattice becomes a two-dimensional (2D) net in which the uniform chains made up of the J_3 interactions are linked by the J_1 interactions forming hexagonal rings (Fig. 4). This 2D spin lattice is again far from the isolated spin dimer model used to describe the magnetic susceptibility of $NH_4CuPO_4 \cdot H_2O$.

Table 2
Exponents ζ_i and valence shell ionization potentials H_{ii} of Slater-type orbitals χ_i used for extended Hückel tight-binding calculation[a]

Atom	χ_I	H_{ii} (eV)	ζ_1	c_1	ζ_2	c_2
Cu	4*s*	−11.0	2.151	1.00		
Cu	4*p*	−6.06	1.370	1.00		
Cu	3*d*	−14.0	7.025	0.4473	3.004	0.6968
P	3*s*	−18.6	2.367	0.5846	1.499	0.5288
P	3*p*	−14.0	2.065	0.4908	1.227	0.5940
O	2*s*	−32.3	2.688	0.7076	1.675	0.3745
O	2*p*	−14.8	3.694	0.3322	1.659	0.7448
H	1*s*	−13.6	1.300			

[a] H_{ii}'s are the diagonal matrix elements $\langle \chi_i | H^{\text{eff}} | \chi_i \rangle$, where H^{eff} is the effective Hamiltonian. In our calculations of the off-diagonal matrix elements $H_{ij} = \langle \chi_i | H^{\text{eff}} | \chi_j \rangle$, the weighted formula was used. See: J. Ammeter, H.-B. Bürgi, J. Thibeault, R. Hoffmann, J. Am. Chem. Soc. 100 (1978) 3686.

Table 3
$(\Delta e)^2$ values calculated for the spin exchange paths J_1–J_4 of $NH_4CuPO_4 \cdot H_2O$[a]

	$x = 0.00$	$x = 0.05$	$x = 0.10$
(a) Without (PO_4) bridge			
J_1	1 (0.00)	253 (0.03)	1660 (0.07)
J_2	502 (0.15)	1500 (0.16)	4540 (0.18)
J_3	1790 (0.53)	4670 (0.49)	13900 (0.55)
J_4	3360 (1.00)	9470 (1.00)	25200 (1.00)
(b) With (PO_4) bridge			
J_1	81 (0.07)	894 (0.46)	4160 (1.00)
J_2	11 (0.01)	42 (0.02)	303 (0.07)
J_3	1120 (1.00)	1950 (1.00)	3320 (0.80)
J_4	10 (0.01)	21 (0.01)	21 (0.01)

[a] The $(\Delta e)^2$ values are given in units of $(\text{meV})^2$, and their relative numbers are given in parentheses.

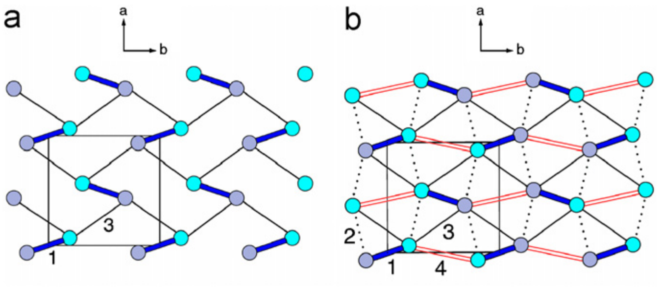

Fig. 4. Spin lattices of $NH_4CuPO_4 \cdot H_2O$ expected from (a) the qualitative spin dimer analysis based on EHTB calculations and (b) the quantitative mapping analysis based on GGA + *U* calculations. The numbers 1–4 represent the spin exchange interactions J_1–J_4, respectively.

Thus, as for the spin lattice responsible for the magnetic properties of $NH_4CuPO_4 \cdot H_2O$, the qualitative analysis based on EHTB calculations provides quite different pictures depending on whether the $(\Delta e)^2$ values are calculated with and without the PO_4 units. To resolve this impasse, the spin exchange interactions of $NH_4CuPO_4 \cdot H_2O$ should be evaluated on the basis of first principles electronic structure calculations. The qualitative spin dimer analysis neglects ferromagnetic contributions to spin exchange and hence cannot predict whether spin exchange interactions will be ferromagnetic or AFM especially when their $(\Delta e)^2$ values are small in magnitude. To provide a quantitative prediction for such cases, first principles electronic structure calculations are necessary.

4. Quantitative mapping analysis of spin exchange interactions

In this section we evaluate the J_1–J_4 parameters on the basis of first principles DFT electronic band structure calculations by first calculating the total energies of several ordered spin states of $NH_4CuPO_4 \cdot H_2O$ and then relating the energy differences between these states to the corresponding energy differences expected from the spin Hamiltonian expressed in terms of the spin exchange parameters J_1–J_4. Since there are four parameters to determine, at least five different ordered spin states are necessary for this mapping analysis. Fig. 5 depicts the six ordered spin arrangements, i.e., the FM, AF1, AF2, AF3, AF4 and AF5 states, employed for our calculations. The total energies of these states were calculated by performing spin-polarized DFT electronic band structure calculations with the projected augmented-wave method encoded in the Vienna ab initio simulation package [14]. Our calculations employed the generalized gradient approximation (GGA) of Perdew et al. [15] for the exchange and correlation correction, the plane wave cutoff energy of 400 eV, and the sampling of the irreducible Brillouin zone with 72 k-points. It has been known that DFT calculations do not properly account for strong correlation effects of magnetic solids [16]. This deficiency of DFT calculations is empirically corrected by introducing either on-site repulsion U [17] or hybrid functional [18]. In the present work the strong correlation effects in $NH_4CuPO_4 \cdot H_2O$ were treated by carrying out GGA plus on-site repulsion (GGA + U) calculations in which the on-site repulsion U was included on copper according to the Duradev et al.'s method [17a]. To see how the value of U affects our results, our calculations were carried out for $U = 5$, 6 and 7 eV.

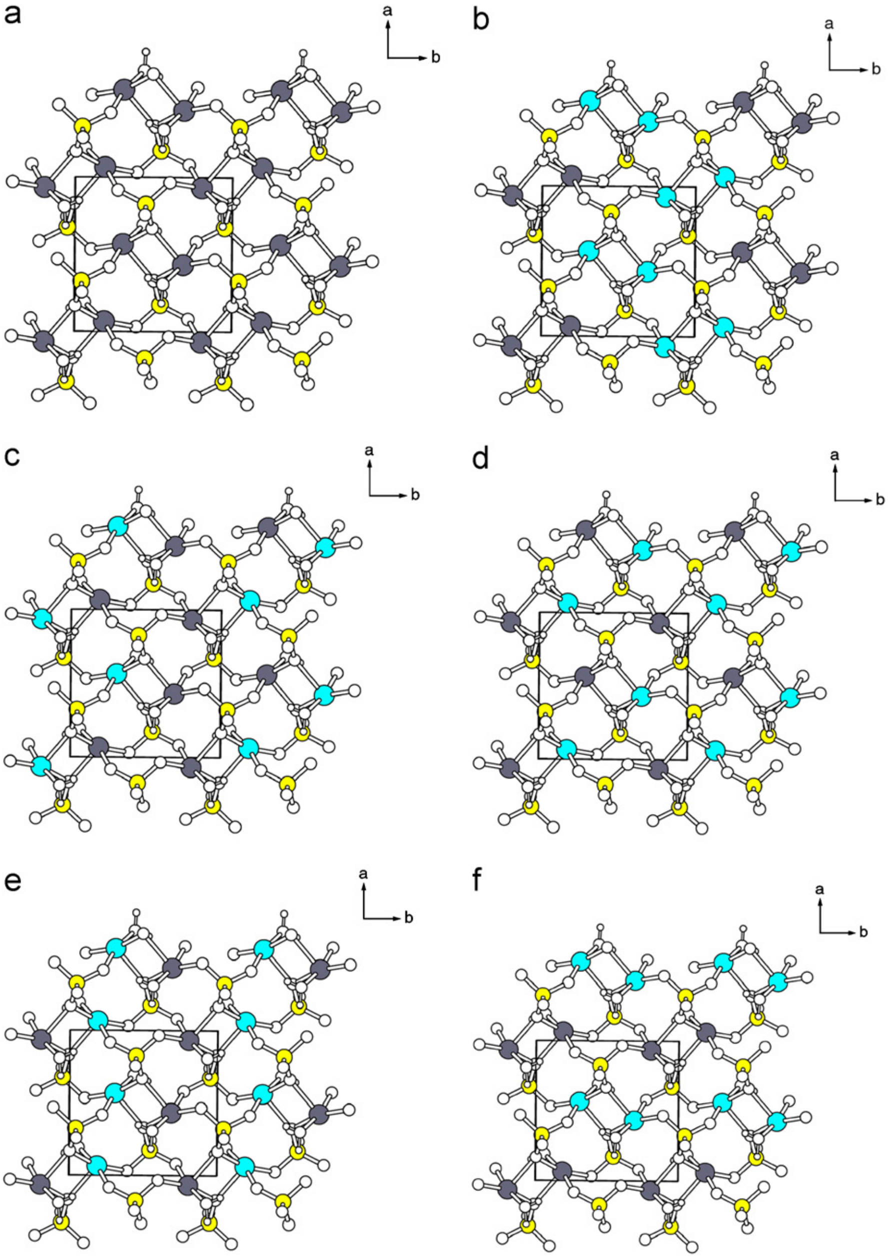

Fig. 5. Ordered spin states FM, AF1, AF2, AF3, AF4 and AF5 of $NH_4CuPO_4 \cdot H_2O$. The gray and cyan circles represent the up and down spin Cu atoms, respectively.

Table 4
Relative energies of the six ordered spin states and values of the four spin exchange parameters of $NH_4CuPO_4 \cdot H_2O$ determined by GGA + U calculations

State	$U = 5$ eV	$U = 6$ eV	$U = 7$ eV
(a) Relative energies (in meV per eight formula units)			
FM	4.33	3.54	2.88
AF1	6.99	5.66	4.50
AF2	0.00	0.00	0.00
AF3	6.60	5.25	4.08
AF4	1.65	1.35	1.08
AF5	1.07	0.90	0.77
(b) Calculated spin exchange parameters (in meV) and calculated Curie–Weiss temperature (in K)			
J_1	−1.39	−1.15	−0.94
J_2	0.21	0.16	0.11
J_3	−1.03	−0.82	−0.64
J_4	2.11	1.68	1.31
θ_{cal}[a]	−2.64	−2.28	−1.96

[a] $\theta_{\mathrm{cal}} = \dfrac{J_1 + 2J_2 + 2J_3 + J_4}{4k_B}$.

Our GGA + U calculations show that the AF2 state is the most stable state. The relative energies calculated for the FM, AF1, AF2, AF3, AF4 and AF5 states are listed in Table 4a. To extract the values of the spin exchange parameters J_1–J_4 from the above electronic structure calculations, we express the total spin exchange interaction energies of the four ordered spin states in terms of the Ising spin Hamiltonian

$$\hat{H} = -\sum_{i<j} J_{ij} \hat{S}_{iz} \hat{S}_{jz}, \tag{2}$$

where J_{ij} ($= J_1$, J_2 or J_3) is the spin exchange parameter for the spin exchange interaction between the spin sites i and j, while $\hat{S}_{iz}$ and $\hat{S}_{jz}$ are the z-components of the spin angular momentum operators at the spin sites i and j, respectively. Then, by applying the energy expressions obtained for spin dimers with N unpaired spins per spin site (in the present case, $N = 1$) [19], the total spin exchange energies per eight formula units are written as

$$E_{\mathrm{FM}} = (-4J_1 - 8J_2 - 8J_3 - 4J_4)(N^2/4), \tag{3a}$$

$$E_{\mathrm{AF1}} = (-4J_1 + 4J_4)(N^2/4), \tag{3b}$$

$$E_{\mathrm{AF2}} = (4J_1 - 4J_4)(N^2/4), \tag{3c}$$

$$E_{\mathrm{AF3}} = (4J_1 + 8J_2 - 8J_3 + 4J_4)(N^2/4), \tag{3d}$$

$$E_{\mathrm{AF4}} = (4J_1 - 8J_2 + 8J_3 + 4J_4)(N^2/4), \tag{3e}$$

$$E_{\mathrm{AF5}} = (-4J_1 + 8J_2 + 8J_3 - 4J_4)(N^2/4). \tag{3f}$$

Thus, from the above equations, the spin exchange parameters J_1–J_4 can be expressed in terms of state energy differences as follows:

$$J_2 = \frac{1}{32}\left(\frac{4}{N^2}\right)\{(E_{\mathrm{AF3}} - E_{\mathrm{AF4}}) - (E_{\mathrm{FM}} - E_{\mathrm{AF5}})\}, \tag{4}$$

$$J_3 = -\frac{1}{16}\left\{(E_{\mathrm{AF3}} - E_{\mathrm{AF4}})\left(\frac{4}{N^2}\right) - 16J_2\right\}, \tag{5a}$$

$$J_3 = -\frac{1}{16}\left\{(E_{\mathrm{FM}} - E_{\mathrm{AF5}})\left(\frac{4}{N^2}\right) - 16J_2\right\}, \tag{5b}$$

$$J_4 = -\frac{1}{16}\left\{[(E_{\mathrm{FM}} - E_{\mathrm{AF4}}) - (E_{\mathrm{AF1}} - E_{\mathrm{AF2}})]\left(\frac{4}{N^2}\right) + 16J_3\right\}, \tag{6a}$$

$$J_4 = -\frac{1}{16}\left\{[(E_{\mathrm{FM}} - E_{\mathrm{AF3}}) - (E_{\mathrm{AF1}} - E_{\mathrm{AF2}})]\left(\frac{4}{N^2}\right) + 16J_2\right\}, \tag{6b}$$

$$J_1 = \frac{1}{16}\left\{[(E_{\mathrm{AF4}} - E_{\mathrm{AF5}}) - (E_{\mathrm{AF1}} - E_{\mathrm{AF2}})]\left(\frac{4}{N^2}\right) + 16J_2\right\}, \tag{7a}$$

$$J_1 = \frac{1}{16}\left\{[(E_{\mathrm{AF3}} - E_{\mathrm{AF5}}) - (E_{\mathrm{AF1}} - E_{\mathrm{AF2}})]\left(\frac{4}{N^2}\right) + 16J_3\right\}. \tag{7b}$$

Note that J_1 and J_3 can be determined from more than one expression. Our calculations show that the different expressions lead to the same result, thereby showing their consistency.

The J_1–J_4 values calculated from the above expressions are summarized in Table 4b. For $U = 6$ eV, the two strongest spin exchange interactions are J_1 and J_4. J_1 is AFM while J_4 is ferromagnetic, and these two interactions form AFM to ferromagnetic (AF–F) alternating chains along the b-direction (Fig. 4b). These chains interact by the spin exchange interactions J_2 and J_3, and these interchain interactions are frustrated (Fig. 4b). Since the J_2 and J_3 interactions are weaker than the J_1 and J_4 interactions, the magnetic properties of $NH_4CuPO_4 \cdot H_2O$ should be, to a first approximation, described by an AF–F alternating chain. Such a chain is known to have a spin gap [5]. The spin exchange parameters obtained for $U = 5$ and 7 eV exhibit trends similar to those found for $U = 6$ eV. Thus, our analysis suggests that an AF–F alternating chain model is more appropriate from the viewpoint of the electronic structure consideration.

To test if the calculated J_1–J_4 parameters are reasonable, we calculate the Curie–Weiss temperature θ, which is derived from susceptibility data in the high temperature region. According to the mean field theory [20], which is valid in the paramagnetic limit, θ is related to the spin exchange parameters as follows:

$$\theta = \frac{S(S+1)}{3k_B} \sum_i z_i J_i, \tag{8a}$$

where the summation runs over all nearest neighbors of a given spin site, z_i is the number of nearest neighbors connected by the spin exchange parameter J_i, and S is the spin quantum number of each spin site (i.e., $S=\frac{1}{2}$ in the present case). Thus, for $NH_4CuPO_4 \cdot H_2O$

$$\theta = \frac{J_1 + 2J_2 + 2J_3 + J_4}{4k_B}. \tag{8b}$$

The θ values estimated by using the spin exchange parameters obtained from the GGA + U calculations, summarized in Table 4b, are in good agreement with the experimental value of -2.7 K. Thus, the present analysis of spin exchange interactions based on GGA + U calculations is highly reliable.

5. Concluding remarks

The quantitative mapping analysis based on the present GGA + U calculations indicates that, to a first approximation, the magnetic properties of $NH_4CuPO_4 \cdot H_2O$ should be described by an AF–F alternating chain model, although an isolated AFM dimer model has been considered to be correct. The qualitative spin dimer analysis based on EHTB calculations is unable to reach this conclusion because the ferromagnetic contributions to the spin exchange interactions are neglected in this approach.

Acknowledgments

The work at NCSU was supported by the Office of Basic Energy Sciences, Division of Materials Sciences, US Department of Energy, under Grant DE-FG02-86ER45259.

References

[1] A. Pujana, J.L. Pizarro, L. Lezama, A. Goñi, M.I. Arriortua, T. Rojo, J. Chem. Mater. 8 (1998) 1055.
[2] E. Burkholder, N.G. Armatas, V. Golub, C.J. O'Connor, J. Zubieta, J. Solid State Chem. 178 (2005) 3145.
[3] (a) D.T. Tran, X. Fan, D.P. Brennan, P.Y. Zavalij, S.R.J. Oliver, Inorg. Chem. 44 (2005) 6192;
  (b) D.T. Tran, X. Fan, D.P. Brennan, P.Y. Zavalij, S.R.J. Oliver, Inorg. Chem. 45 (2006) 7027.
[4] H.-J. Koo, C. Lee, G.B. Wilson-Short, D. Dai, M.-H. Whangbo, Inorg. Chem. 46 (2007) 2498.
[5] Y. Miura, R. Hirai, Y. Kobayashi, M. Sato, J. Phys. Soc. Jpn. 75 (2006) 84707.
[6] (a) M.-H. Whangbo, H.-J. Koo, D. Dai, J. Solid State Chem. 176 (2003) 417;
  (b) M.-H. Whangbo, D. Dai, H.-J. Koo, Solid State Sci. 7 (2005) 827.
[7] (a) H.-J. Koo, M.-H. Whangbo, Inorg. Chem. 40 (2001) 2169;
  (b) H.-J. Koo, M.-H. Whangbo, P.D. VerNooy, C.C. Torardi, W.J. Marshall, Inorg. Chem. 41 (2002) 4664;
  (c) M.-H. Whangbo, H.-J. Koo, D. Dai, D. Jung, Inorg. Chem. 42 (2003) 3898;
  (d) H.-J. Koo, M.-H. Whangbo, K.-S. Lee, Inorg. Chem. 42 (2003) 5932;
  (e) H.-J. Koo, D. Dai, M.-H. Whangbo, Inorg. Chem. 44 (2005) 4359.
[8] J.B. Goodenough, Magnetism and the Chemical Bond, Wiley, Cambridge, MA, 1963.
[9] (a) F. Illas, I. de P. R. Moreira, C. de Graaf, V. Barone, Theor. Chem. Acc. 104 (2000) 265 and the references cited therein;
  (b) E. Ruiz, A. Rodriguez-Fortea, J. Cano, S. Alvarez, J. Phys. Chem. Solids 65 (2004) 799.
[10] (a) A. Chartier, P. D'Arco, R. Dovesi, V.R. Saunders, Phys. Rev. B 60 (1999) 14042 and the references cited therein;
  (b) D. Dai, M.-H. Whangbo, H.-J. Koo, X. Rocquefelte, S. Jobic, A. Villesuzanne, Inorg. Chem. 44 (2005) 2407.
[11] (a) P.J. Hay, J.C. Thibeault, R. Hoffmann, J. Am. Chem. Soc. 97 (1975) 4884;
  (b) O. Kahn, Molecular Magnetism, VCH Publisher, Weinheim, 1993.
[12] (a) R. Hoffmann, J. Chem. Phys. 39 (1963) 1397;
  (b) Our calculations were carried out by employing the CAESAR 2.0 (Crystal and Electronic Structure Analyzer) program package (This program can be downloaded free of charge from the website, 〈http://chvamw.chem.ncsu.edu/〉).
[13] E. Clementi, C. Roetti, At. Data Nucl. Data Tables 14 (1974) 177.
[14] (a) G. Kresse, J. Hafner, Phys. Rev. B 62 (1993) 558;
  (b) G. Kresse, J. Furthmüller, Comput. Mater. Sci. 6 (1996) 15;
  (c) G. Kresse, J. Furthmüller, Phys. Rev. B 54 (1996) 11169.
[15] J.P. Perdew, S. Burke, M. Ernzerhof, Phys. Rev. Lett. 77 (1996) 3865.
[16] (a) R. Martin, F. Illas, Phys. Rev. Lett. 79 (1997) 1539;
  (b) I.d.P.R. Moreira, F. Illas, Phys. Rev. B 60 (1999) 5179.
[17] (a) S.L. Dudarev, G.A. Botton, S.Y. Savrasov, C.J. Humphreys, A.P. Sutton, Phys. Rev. B 57 (1998) 1505;
  (b) (b)V.I. Anisimov, I.V. Solovyev, M.A. Korotin, M.T. Czyzyk, G.A. Sawatzky, Phys. Rev. B 48 (1993) 16929;
  (c) M.T. Czyzyk, G.A. Sawatzky, Phys. Rev. B 49 (1994) 14211.
[18] (a) I.d.P.R. Moreira, F. Illas, Phys. Rev. B 65 (2002) 155102;
  (b) X. Feng, N.M. Harrison, Phys. Rev. B 70 (2004) 092402.
[19] (a) D. Dai, M.-H. Whangbo, J. Chem. Phys. 114 (2001) 2887;
  (b) D. Dai, M.-H. Whangbo, J. Chem. Phys. 118 (2003) 29.
[20] J.S. Smart, Effective Field Theory of Magnetism, Saunders, Philadelphia, 1966.